scientific reports

Check for updates

OPEN

Characterization of alternative mRNA splicing in cultured cell populations representing progressive stages of human fetal kidney development

Yishay Wineberg[1,6], Itamar Kanter[1,6], Nissim Ben-Haim[1,6], Naomi Pode-Shakked[2,3,4,6], Efrat Bucris[1], Tali Hana Bar-Lev[1], Sarit Oriel[1], Harel Reinus[1], Yishai Yehuda[1], Rotem Gershon[2,3,4], Rachel Shukrun[2,4], Dekel Dov Bar-Lev[2,3], Achia Urbach[5], Benjamin Dekel[2,3,4,7] & Tomer Kalisky[1,7]✉

Nephrons are the functional units of the kidney. During kidney development, cells from the cap mesenchyme—a transient kidney-specific progenitor state—undergo a mesenchymal to epithelial transition (MET) and subsequently differentiate into the various epithelial cell types that create the tubular structures of the nephron. Faults in this transition can lead to a pediatric malignancy of the kidney called Wilms' tumor that mimics normal kidney development. While human kidney development has been characterized at the gene expression level, a comprehensive characterization of alternative splicing is lacking. Therefore, in this study, we performed RNA sequencing on cell populations representing early, intermediate, and late developmental stages of the human fetal kidney, as well as three blastemal-predominant Wilms' tumor patient-derived xenografts. Using this newly generated RNAseq data, we identified a set of transcripts that are alternatively spliced between the different developmental stages. Moreover, we found that cells from the earliest developmental stage have a mesenchymal splice-isoform profile that is similar to that of blastemal-predominant Wilms' tumor xenografts. RNA binding motif enrichment analysis suggests that the mRNA binding proteins ESRP1, ESRP2, RBFOX2, and QKI regulate alternative mRNA splicing during human kidney development. These findings illuminate new molecular mechanisms involved in human kidney development and pediatric kidney cancer.

Kidney development occurs during the embryonic stage from week 5 to week 36 of gestation in humans[1–3]. It starts as an interaction between two lineages that originate from the intermediate mesoderm: the nephric duct—an epithelial tubular structure, and the metanephric mesenchyme—which is composed of loosely connected mesenchymal cells. This interaction causes the nephric duct to invade the metanephric mesenchyme and, through a series of bifurcations, create a tree-like structure called the ureteric tree. The tips of this tree induce the surrounding cells of the metanephric mesenchyme to condense and form the "cap mesenchyme", which is the nephron progenitor cell (NPC) population. Cells of the cap mesenchyme then undergo a mesenchymal to epithelial transition (MET) to create early epithelial structures called pre-tubular aggregates. These, in turn, progressively differentiate and elongate through a series of intermediate structures (renal vesicles, comma-shaped, and S-shaped bodies) to eventually give rise to the various epithelial tubular segments of the mature nephron.

[1]Department of Bioengineering and Bar-Ilan Institute of Nanotechnology and Advanced Materials (BINA), Bar-Ilan University, 52900 Ramat Gan, Israel. [2]Pediatric Stem Cell Research Institute, Edmond and Lily Safra Children's Hospital, Sheba Medical Center, 52621 Tel-Hashomer, Israel. [3]Division of Pediatric Nephrology, Sheba Medical Center, 52621 Tel-Hashomer, Israel. [4]Sackler Faculty of Medicine, Tel-Aviv University, 69978 Tel-Aviv, Israel. [5]The Mina and Everard Goodman Faculty of Life Sciences, Bar-Ilan University, 52900 Ramat-Gan, Israel. [6]These authors contributed equally: Yishay Wineberg, Itamar Kanter, Nissim Ben-Haim and Naomi Pode-Shakked. [7]These authors jointly supervised this work: Benjamin Dekel and Tomer Kalisky. ✉email: tomer.kalisky@biu.ac.il

Wilms' tumor (WT) is the most common pediatric tumor of the kidney, with 75% of cases diagnosed in children under the age of five[1,4,5]. It is thought that Wilms' tumors originate from fetal developing tissues that failed to differentiate properly. As a result, Wilms' tumor is considered a model system for understanding the link between normal development and tumorigenesis. In many cases Wilms' tumors contain three cellular components that appear in varying proportions between different patients and that mimic the three main stages of normal nephrogenic differentiation: the stroma—corresponding to the un-induced metanephric mesenchyme, the blastema—corresponding to the cap mesenchyme, and disordered non-functional epithelia that resemble the early epithelial structures of the fetal kidney. The blastema is thought to represent the least differentiated and most malignant component of the tumor and, typically, Wilms' tumors with blastemal-predominance (after preoperative chemotherapy) require more aggressive treatment[6].

In a recent study (Pode-Shakked et al.[7]) we found that cells from different developmental stages can be isolated from cultured human fetal kidney (hFK) cells using a combination of two surface markers: NCAM1, a cell adhesion protein that is overexpressed in the cap mesenchyme and early epithelial structures, and CD133 (PROM1), a membrane-bound protein which marks the more mature epithelial structures. We showed that a combination of those two markers allows for isolating cells from progressive stages of human fetal kidney development: the NCAM1+/CD133− cell fraction (which we denote "hFK1") enriches for cells in the early renal developmental stages, mainly the cap mesenchyme; the NCAM1+/CD133+ cell fraction ("hFK2") enriches for cells in an intermediate state corresponding to early renal epithelial structures; and the NCAM1−/CD133+ cell fraction ("hFK3") enriches for cells at a more advanced differentiation state of the renal tubular epithelium.

To characterize these three cell fractions, we previously[7] performed RNA sequencing and qPCR. In hFK1 (the NCAM1+/CD133− cell fraction) we observed a strong expression of genes that were previously found to be overexpressed in the cap mesenchyme and in the un-induced metanephric mesenchyme (e.g. SIX2, SALL2, OSR1, and CDH11). Likewise, in hFK2 (the NCAM1+/CD133+ cell fraction) we observed an upregulation of genes related to epithelial differentiation (e.g. CDH1 and EPCAM), and even more in hFK3 (the NCAM1−/CD133+ cell fraction). This gradual pattern of switching from mesenchymal to epithelial characteristics, was further supported by splice isoform switching in the genes ENAH, CD44, and CTNND1, from their typical mesenchymal to epithelial isoforms, similar to what was previously observed in epithelial-mesenchymal transition (EMT) in embryonic development and metastatic breast cancer[8–12]. In a subsequent study[13] we used single-cell qPCR to confirm the splice isoform switching in the gene ENAH at the single-cell level. Moreover, we observed a strong over-expression of the mesenchymal isoform of ENAH in a blastemal-predominant Wilms' tumor patient-derived xenograft (WT-PDX).

Although in those previous studies[7,13] we were able to find alternative splicing in specific genes, the RNA sequencing that we performed was originally designed for gene expression (50 bp, single-end, at approximately 20 million reads per sample) and was less suitable for analysis of alternative splicing. We, therefore, present here a more comprehensive and quantitative study of the alternative splicing taking place in the developing human fetal kidney and in Wilms' tumors. To achieve this, we re-sequenced the three cell fractions of the human fetal kidney (hFK1, hFK2, and hFK3) paired-end (2 × 126 bases) and more deeply (at approximately 40 million paired-end reads per sample). In addition, we also sequenced three additional samples of blastemal-predominant Wilms' tumor xenografts that were derived from three different patients (WT11, WT14, and WT37)[7,13–16] (Fig. 1).

Materials and methods

Tissue collection, dissociation, culturing, and flow cytometry. In this study we characterized alternative splicing in three cell populations from the human fetal kidney (hFK1: NCAM1+/CD133−, hFK2: NCAM1+/CD133+, and hFK3: NCAM1−/CD133+) that we have shown in a previous study[7] to represent progressive developmental stages of the human fetal kidney. In that study[7], we performed RNA sequencing that was designed for gene expression analysis (50 bp, single-end, at approximately 20 million reads per sample) and was less suitable for comprehensive analysis of alternative splicing. We, therefore, re-sequenced the three cell fractions paired-end (2 × 126 bases) and more deeply (at approximately 40 million paired-end reads per sample). In addition, we also sequenced three additional RNA samples of blastemal-predominant Wilms' tumor xenografts (WT-PDX) that were derived from three different patients (WT11, WT14, and WT37). These RNA samples were collected in the course of previous studies[7,13–16] that were performed beforehand in the Pediatric Stem Cell Research Institute at the Sheba Medical Center. Details of tissue collection can be found in the above references, while below we describe them briefly.

Human fetal kidney cells were collected as previously described[7,13] (Fig. 1). Briefly, kidneys were collected from elective abortions at fetal gestational age between 15 to 19 weeks. The kidneys were dissociated into single-cell suspensions, resuspended in serum-free medium (SFM), plated in flasks, and cultured until reaching 80% confluence. FACS was used to isolate three cell fractions representing progressive developmental stages of the human fetal kidney: hFK1 (NCAM1+/CD133−), hFK2 (NCAM1+/CD133+), and hFK3 (NCAM1−/CD133+), as previously described[7]. All assays were conducted with low passage cultured cells (passage 0). Likewise, Wilms' tumor patient-derived xenografts (WT-PDX) were established, propagated in mice, and collected as previously described[7,15] (Fig. 1). The xenografts were then dissociated into single-cell suspensions, resuspended in serum-containing medium (SCM), plated in flasks, and cultured overnight. For this study we used three blastemal-predominant Wilms' tumor xenografts (WT-PDX) originating from three different patients (WT11, WT14, and WT37).

All experiments were performed in accordance with relevant guidelines and regulations. All human tissue handling procedures were approved by the local ethical committee of the Sheba Medical Center and informed consent was given by the legal guardians of the patients involved according to the Declaration of Helsinki. All

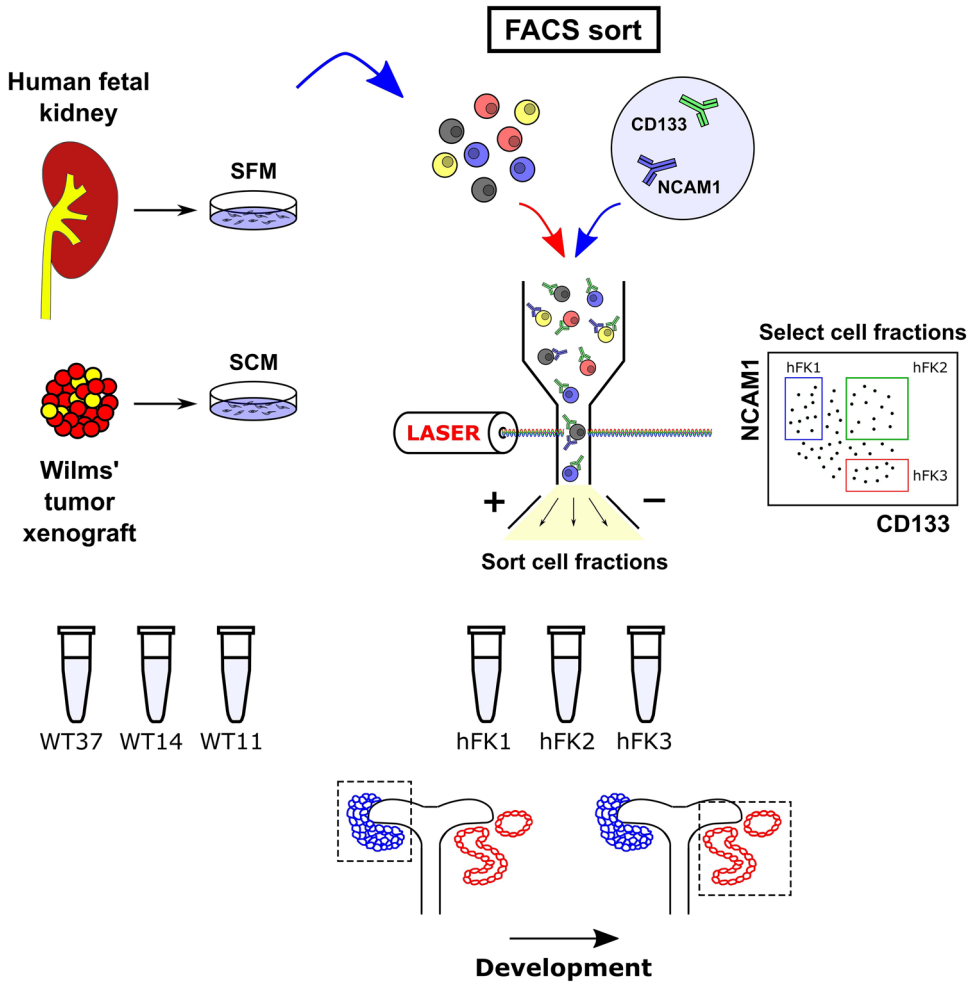

Figure 1. A sketch of the experiments performed to obtain the RNA samples that were analyzed in this study (see also Pode-Shakked et al.[7]). Cells from a human fetal kidney (hFK) were cultured overnight in serum-free medium (SFM) which was found to help preserve a small population of undifferentiated cells. The cells were then dissociated and sorted by FACS to enrich for cell fractions representing three progressive renal developmental stages: NCAM-high/CD133-low ("hFK1"), a cell population that was previously found to be enriched for immature cells from early renal developmental stages, mainly the cap mesenchyme; NCAM-high/CD133-high ("hFK2"), an intermediate state, presumably enriched for cells representing early epithelial structures; and NCAM-low/CD133-high ("hFK3"), a population enriched for more differentiated epithelial cells. In parallel, cells from three blastemal-predominant Wilms' tumor patient-derived xenografts ("WT11", "WT14", and "WT37") were cultured overnight in serum-containing medium (SCM). RNA from all samples was extracted and deeply sequenced paired-end.

animal procedures were approved by the Institutional Animal Care and Use Committee in the Sheba Medical Center. Likewise, the study was carried out in compliance with the ARRIVE guidelines (https://arriveguidelines.org).

RNA purification and sequencing. Bulk total RNA was prepared from ~ $1.5 * 10^5$ cells using the Direct-zol RNA MiniPrep kit (R2050, Zymo Research) according to the manufacturer's instructions and stored in − 80 °C. RNA was quantified on an Agilent BioAnalyzer (Agilent Technologies) and aliquots of 270–500 ng were made into cDNA libraries using the TruSeq mRNA-Seq library kit (Illumina).

All 6 libraries (hFK1, hFK2, hFK3, WT11, WT14, and WT37) were sequenced paired-end 2 × 126 bases on an Illumina HiSeq 2500 platform in the Israel National Center for Personalized Medicine (G-INCPM). For each sample we obtained approximately 40 million paired-end reads.

RNA sequence data preprocessing and gene expression analysis. Raw reads were aligned by TopHat2[17] to the human hg19 genome. Aligned reads were counted by HTSeq[18]. Data normalization (resulting in a matrix of normalized gene expression counts), estimation of size factors, and differential gene expression were done by DESeq2[19].

The GEO series record for the RNA sequencing data is: GSE150684.

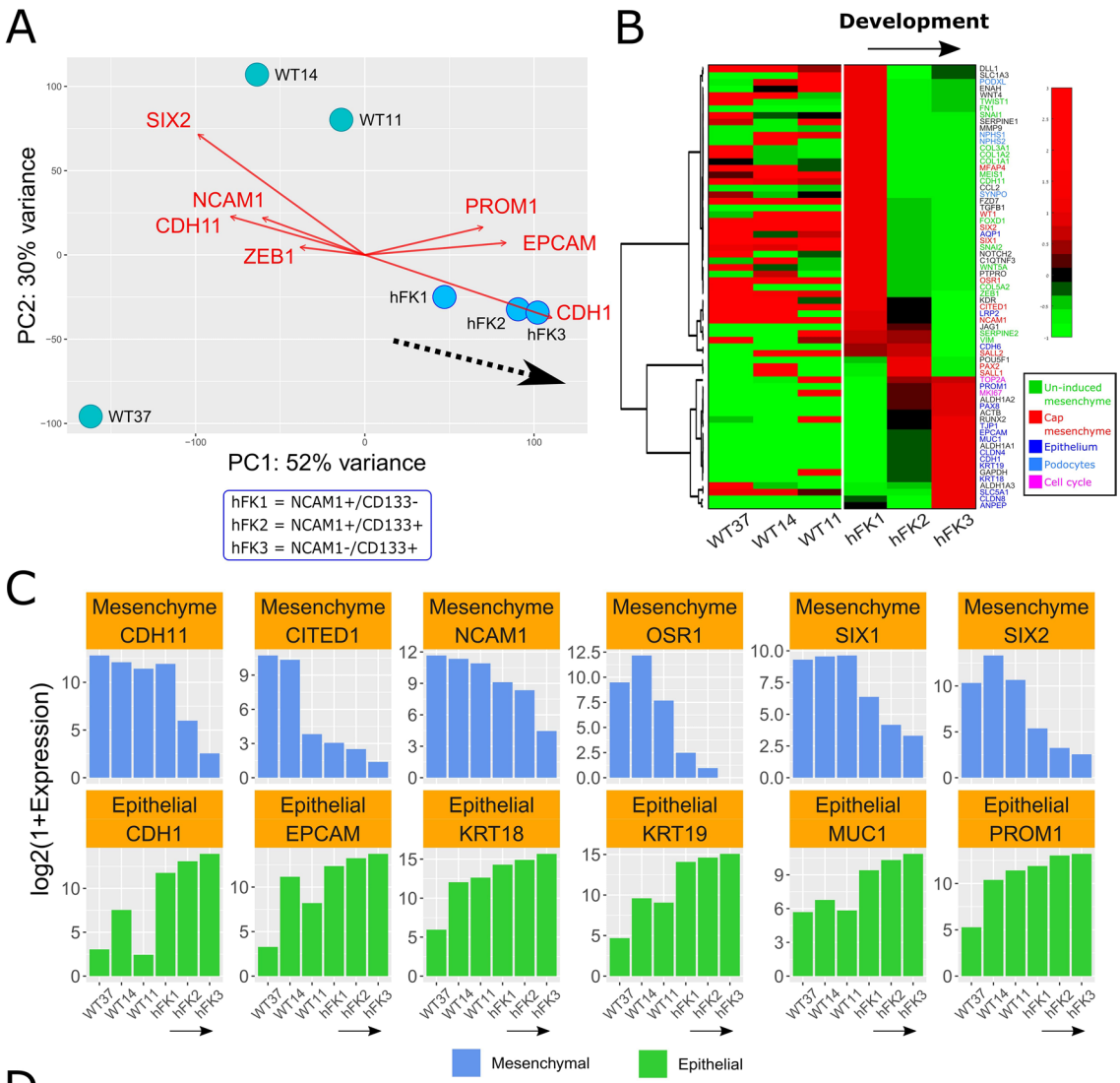
A
WT14
WT11
SIX2
NCAM1
CDH11
PROM1
EPCAM
ZEB1
hFK1
hFK2
hFK3
CDH1
WT37
PC2: 30% variance
PC1: 52% variance
hFK1 = NCAM1+/CD133-
hFK2 = NCAM1+/CD133+
hFK3 = NCAM1-/CD133+
B
Development
Un-induced mesenchyme
Cap mesenchyme
Epithelium
Podocytes
Cell cycle
WT37
WT14
WT11
hFK1
hFK2
hFK3
C
log2(1+Expression)
Mesenchyme CDH11
Mesenchyme CITED1
Mesenchyme NCAM1
Mesenchyme OSR1
Mesenchyme SIX1
Mesenchyme SIX2
Epithelial CDH1
Epithelial EPCAM
Epithelial KRT18
Epithelial KRT19
Epithelial MUC1
Epithelial PROM1
Mesenchymal
Epithelial
D
-log10(q_value Bonferroni)
Epithelial cell differentiation
Epithelium development
Cell-cell junction
Cell adhesion
Cell adhesion molecules (CAMs)
Cell adhesion molecule binding
Cell junction organization
Cell junction
CDH1 interactions
Cell-cell adhesion
Apical part of cell
Apical junction complex
Apical plasma membrane
Tight junction
Cell junction organization
Cell-cell junction organization
Cadherin binding
Epithelial cell development
Regulation of cell-cell adhesion
Enrichment plot:
HALLMARK_EPITHELIAL_MESENCHYMAL_TRANSITION
Enrichment score (ES)
Overexpressed in hFK3
Overexpressed in hFK1
Ranked list metric (PreRanked)
Rank in Ordered Dataset
Enrichment profile
Hits
Ranking metric scores

◂**Figure 2.** RNA sequencing identifies a set of genes that are differentially expressed between the early, intermediate, and late developmental stages of the human fetal kidney, where cells at the early stage of human kidney development (NCAM-high/CD133-low, hFK1) have a mesenchymal gene expression profile that is similar to that observed in blastemal-predominant Wilms' tumor patient-derived xenografts (WT-PDX). (**A**) A PCA biplot of gene expression levels. The three human fetal kidney cell fractions (hFK1, hFK2, and hFK3) lie on a trajectory (dotted black arrow) along which the epithelial-associated genes (CDH1, EPCAM, and PROM1 [=CD133]) increase and mesenchymal-associated genes (CDH11, ZEB1, NCAM1, SIX2) decrease. Note the large spread of Wilms' tumor xenografts in gene expression space, which indicates a large variability between tumors from different patients. (**B**) Hierarchical clustering of 67 selected genes that were previously found to be related to kidney development. It can be seen that the blastemal-predominant Wilms' tumor patient-derived xenografts (WT37, WT14, and WT11) are similar to hFK1—the cell fraction that represents the most immature fraction of the human fetal kidney—in that they overexpress mesenchymal related genes and under-express epithelial related genes. The order of genes and the dendrogram were determined by hierarchical clustering of the human fetal kidney samples only (hFK1, hFK2, and hFK3). Note that although most epithelial associated genes that are over-expressed in hFK3, the podocyte markers PODXL, NPHS1/2, and SYNPO are only high in the early developmental stages (hFK1) and decrease with differentiation to hFK2 and hFK3. This is probably due to the fact podocytes cannot be cultured in the serum-free media that was used to culture the hFK cells. (**C**) Barplots of selected mesenchymal and epithelial associated genes involved in kidney development show sequential decrease in mesenchymal-associated genes and sequential increase in epithelial-associated genes in the fetal kidney samples (hFK1, hFK2, and hFK3), whereas the three Wilms' tumor xenografts (WT11, WT14, and WT37) all have high expression of mesenchymal associated genes and relatively low expression of epithelial-associated genes. (**D**) Gene Ontology (GO) enrichment analysis for 395 genes that were upregulated at least twofold (log2foldChange > 1) in hFK3 (the mature fetal developmental fraction) with respect to hFK1, WT11, WT14, and WT37 (see Fig. S1) shows that they are related to epithelial differentiation (see Table S2). Likewise, Gene Set Enrichment Analysis (GSEA) showed that genes that are over-expressed in the early developmental cell fraction hFK1 (with respect to late fraction hFK3) are related to the Epithelial to Mesenchymal transition (EMT).

Heatmaps, PCA biplots, and barplots were performed in Matlab (Mathworks) and R. Gene Ontology (GO) enrichment analysis was done with ToppGene (https://toppgene.cchmc.org)[20]. Gene Set Enrichment Analysis (GSEA)[21] was used to check for enrichment of gene sets from the Molecular Signatures Database (MSigDB).

mRNA splicing analysis for identification of alternative splicing events and putative splicing regulators. rMATS[22] was used to detect alternative mRNA splicing events between the cell fractions representing early (hFK1) and late (hFK3) stages of human fetal kidney development, as well as for quantifying inclusion levels in all transcriptomes (Tables S3–S7). Selected splicing events (e.g. cassette exons) were visualized and validated using IGV[23], Sashimi plots[24], and bar plots of inclusion levels obtained from rMATS (supplementary information). For some events we also used DEXSeq[3] to complement rMATS and validate differential expression in specific exons (Table S8).

Gene Ontology (GO) enrichment analysis for the genes containing alternatively spliced cassette exons was done with ToppGene (https://toppgene.cchmc.org)[20].

rMAPS (http://rmaps.cecsresearch.org/)[25] was used to test for enrichment of binding motifs of RNA binding proteins (RBPs) in the vicinity of alternatively spliced cassette exons in order to identify putative splicing regulators.

A list of 89 RNA binding proteins (RBPs) was obtained from the rMAPS website (http://rmaps.cecsresearch.org/Help/RNABindingProtein)[25–27]. Apart from the RNA binding motifs that were tested by the default settings in the rMAPS website, we also tested additional UGG-enriched motifs that were previously found to be binding sites for the RNA binding proteins ESRP1[28,29] and ESRP2[30] (Table S10). For the RNA binding proteins RBFOX1 and RBFOX2, following Yang et al.[31] and the CISBP-RNA database[26] (http://cisbp-rna.ccbr.utoronto.ca) we assumed that both proteins (RBFOX1 and RBFOX2) preferentially bind to the same motif ([AT]GCATG[AC]) on mRNA.

Results

RNA sequencing identifies a set of genes that are differentially expressed between the early, intermediate, and late developmental stages of the human fetal kidney. We sequenced mRNA from three cell fractions collected from a human fetal kidney (hFK) that represent three consecutive renal developmental stages. The cells were cultured overnight in serum-free medium (SFM) which was found to help preserve a small population of undifferentiated cells, and then dissociated and sorted by FACS to enrich for the following cell fractions: NCAM-high/CD133-low ("hFK1"), a population that was previously shown to be enriched for immature cells originating from the cap mesenchyme; NCAM-high/CD133-high ("hFK2"), an intermediate state, presumably consisting of cells representing early developmental epithelial structures; and NCAM-low/CD133-high ("hFK3"), a population consisting of more differentiated epithelial cells. In parallel, cells from three blastemal-predominant Wilms' tumor xenografts (WT-PDX) that were derived from three different patients ("WT11", "WT14", and "WT37") were cultured overnight in serum-containing medium (SCM). RNA from all six samples was extracted, sequenced paired-end 2 × 126 bases at approximately 40 million paired-end reads per sample on an Illumina HiSeq 2500 platform, and analyzed for gene expression and alternative splicing.

For consistency, we first performed gene expression analysis for all samples. Principal Components Analysis (PCA) confirmed that the three fetal fractions (hFK1, hFK2, and hFK3) are sequentially ordered in gene

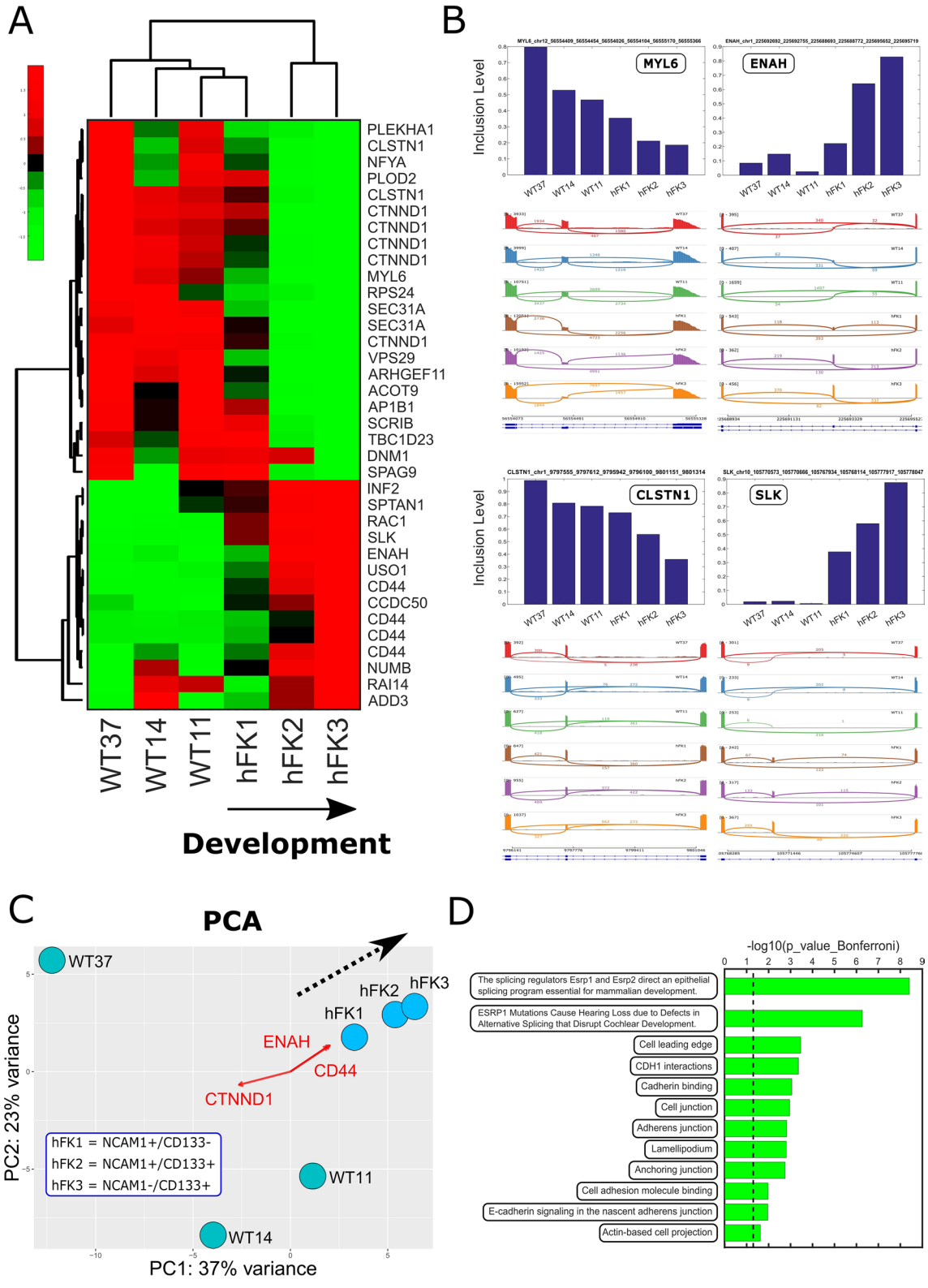
A
PLEKHA1
CLSTN1
NFYA
PLOD2
CLSTN1
CTNND1
CTNND1
CTNND1
CTNND1
MYL6
RPS24
SEC31A
SEC31A
CTNND1
VPS29
ARHGEF11
ACOT9
AP1B1
SCRIB
TBC1D23
DNM1
SPAG9
INF2
SPTAN1
RAC1
SLK
ENAH
USO1
CD44
CCDC50
CD44
CD44
CD44
NUMB
RAI14
ADD3
WT37
WT14
WT11
hFK1
hFK2
hFK3
Development
B
MYL6
ENAH
CLSTN1
SLK
Inclusion Level
C
PCA
WT37
hFK2
hFK3
hFK1
ENAH
CD44
CTNND1
hFK1 = NCAM1+/CD133-
hFK2 = NCAM1+/CD133+
hFK3 = NCAM1-/CD133+
WT11
WT14
PC2: 23% variance
PC1: 37% variance
D
-log10(p_value_Bonferroni)
The splicing regulators Esrp1 and Esrp2 direct an epithelial splicing program essential for mammalian development.
ESRP1 Mutations Cause Hearing Loss due to Defects in Alternative Splicing that Disrupt Cochlear Development.
Cell leading edge
CDH1 interactions
Cadherin binding
Cell junction
Adherens junction
Lamellipodium
Anchoring junction
Cell adhesion molecule binding
E-cadherin signaling in the nascent adherens junction
Actin-based cell projection

◂**Figure 3.** RNA sequencing identifies a set of transcripts that are alternatively spliced between the early, intermediate, and late developmental stages of the human fetal kidney, where cells at the early stage of human kidney development (NCAM-high/CD133-low, hFK1) have a mesenchymal splice-isoform profile that is similar to that observed in blastemal-predominant Wilms' tumor patient-derived xenografts (WT-PDX). (**A**) Hierarchical clustering of the inclusion levels of 36 selected cassette exons that were manually found to be alternatively spliced between hFK1 and hFK3—the two cell populations that represent early (hFK1) and late (hFK3) developmental stages in the fetal human kidney. Note that the late-stage fetal kidney cell fractions hFK2 and hFK3 are grouped in one cluster, whereas hFK1, the early-stage fraction, is grouped with the Wilms' tumor xenograft samples. The 36 cassette exons were selected as follows: We chose cassette exons that were significantly differentially spliced (FDR < 1E−9 and difference in inclusion levels > 0.1) between hFK1 and hFK3, and from these we selected 36 cassette exons that also showed clear alternative splicing by manual inspection in the IGV genome browser. (**B**) Barplots and sashimi plots for selected cassette exons show the change in inclusion levels between the different cell fractions. Exons within the genes MYL6 and CLSTN1 are high in Wilms' tumors and early fetal kidney cells (hFK1) and decrease during kidney development (hFK2 and hFK3), while those within ENAH and SLK are low in Wilms' tumors and early fetal kidney cells (hFK1) and increase during kidney development (hFK2 and hFK3). (**C**) A PCA biplot of exon inclusion levels that were calculated by rMATS. Each point represents a different cell fraction. The three human fetal kidney samples (hFK1, hFK2, and hFK3) lie on a trajectory (dotted black arrow) along which the epithelial-associated exons within the genes CD44 and ENAH sequentially increase, and a mesenchymal-associated exon within the gene CTNND1 sequentially decreases. For PCA analysis we used all cassette exons that were detected by rMATS. (**D**) Gene Ontology (GO) enrichment analysis for the genes containing the 36 selected cassette exons indicates that they are related to mesenchymal or epithelial characteristics (e.g. cell motility and cell to cell junctions) and that alternative splicing in a significant fraction of these genes is regulated by the RNA binding proteins ESRP1 and ESRP2 (see Table S9).

expression space (Fig. 2A), as expected. The three Wilms' tumor xenografts (WT11, WT14, and WT37) are closer to hFK1, the most immature fetal cell fraction, than to the other two fetal cell fractions (hFK2 and hFK3), which indicates that these Wilms' tumors resemble an early stage in fetal kidney development. Likewise, we observed that genes associated with epithelial differentiation (PROM1 (CD133), EPCAM, and CDH1) increase towards hFK3, the cell fraction representing late-stage fetal development, whereas genes associated with the un-induced metanephric mesenchyme (ZEB1), the cap-mesenchyme (SIX2), or both (NCAM1 and CDH11)[13], decrease (Fig. 2A, red arrows). A heatmap of 67 genes that were previously found to be associated with the different cell types that co-exist within the developing kidney[13,32–34] (Fig. 2B), as well as barplots for selected genes associated with renal-mesenchymal and epithelial cell states (Fig. 2C), showed a sequential decrease in mesenchymal-associated genes and an increase in epithelial-associated genes in the fetal kidney samples (hFK1, hFK2, and hFK3), whereas all three Wilms' tumor xenografts (WT11, WT14, and WT37) were observed to have a relatively high expression of mesenchymal associated genes.

Next, we selected a set of 395 genes that were found by intersecting all the gene sets that were upregulated at least twofold (log2foldChange > 1) in hFK3 (the mature fetal developmental fraction) with respect to hFK1, WT11, WT14, and WT37 (see Fig. S1). We performed Gene Ontology (GO) enrichment analysis using ToppGene[20] and found that the genes in this set are related to epithelial differentiation (Fig. 2D, Table S2). Likewise, Gene Set Enrichment Analysis (GSEA)[21] of all genes, ranked according to their fold-change in expression between hFK1 and hFK3, showed that genes that are over-expressed in hFK1 (the early developmental cell fraction) vs. hFK3 (the late developmental cell fraction) are related to the Epithelial to Mesenchymal transition (EMT). All these findings indicate that cells at the early stage of kidney development (hFK1) have a more mesenchymal gene expression profile that is similar to that of the blastemal-predominant Wilms' tumor patient-derived xenografts (WT-PDX) (WT37, WT14, and WT11).

RNA sequencing identifies a set of transcripts that are alternatively spliced between the early, intermediate, and late developmental stages of the human fetal kidney. In order to characterize alternative mRNA splicing associated with the mesenchymal to epithelial transition (MET) that occurs during kidney development, we first inspected the genes ENAH[8–10] (Figs. S2 and S17), CD44[11,12] (Figs. S2 and S13), CTNND1[10,35] (Figs. S2 and S15), FGFR2[35,36] (Figs. S2 and S36), and EPB41L5[10,37] (Figs. S2 and S42), which were previously shown to be alternatively spliced in mesenchymal and epithelial tissues. We found that all three blastemal-predominant Wilms' tumor patient-derived xenografts (WT37, WT14, and WT11) typically express the mesenchymal isoforms of these genes. In the fetal kidney, we found that hFK1—the cell fraction representing the early stage of fetal kidney development—expresses a mixture of both mesenchymal and epithelial isoforms of these genes, whereas the cell fractions representing more differentiated stages (hFK2 and hFK3) predominantly express the epithelial splice isoforms.

We next performed a more comprehensive analysis using rMATS[22], a tool for detecting alternative splicing from RNA sequencing datasets (Tables S3–S7). PCA of exon inclusion levels (Fig. 3C) showed that the three human fetal kidney samples (hFK1, hFK2, and hFK3) lie on a trajectory along which the epithelial-associated exons within the genes CD44 and ENAH sequentially increase and a mesenchymal-associated exon within the gene CTNND1 sequentially decreases. We also observed that the exon inclusion level profiles of the blastemal-predominant Wilms' tumor patient-derived xenografts are typically closer to hFK1—the most immature fetal cell fraction—than to the other more mature fetal cell fractions (hFK2 and hFK3), similar to what we have seen in gene expression (Fig. 2A).

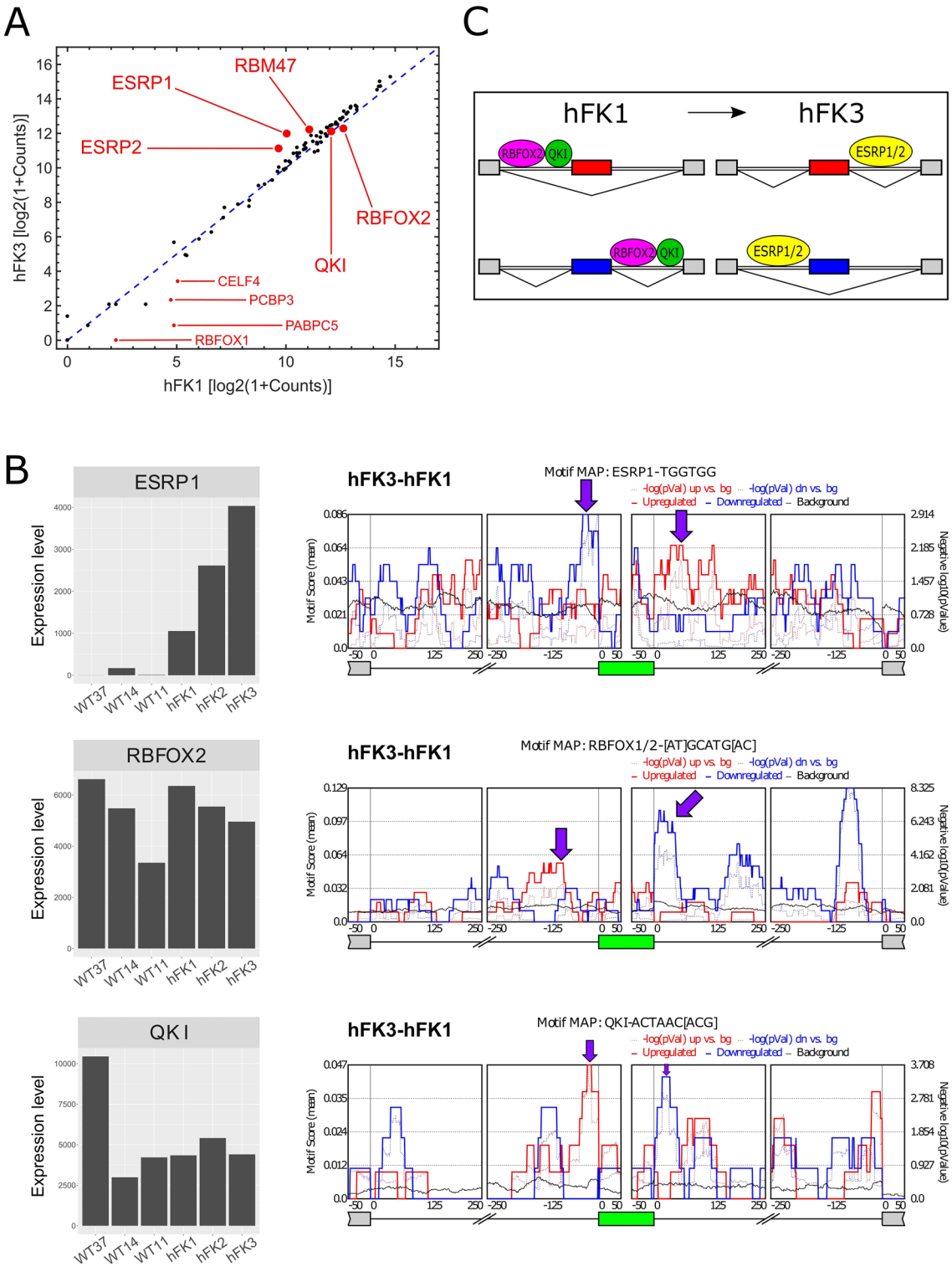
A
ESRP1
RBM47
ESRP2
RBFOX2
QKI
CELF4
PCBP3
PABPC5
RBFOX1
hFK3 [log2(1+Counts)]
hFK1 [log2(1+Counts)]
C
hFK1
hFK3
RBFOX2
QKI
ESRP1/2
B
ESRP1
RBFOX2
QKI
Expression level
WT37
WT14
WT11
hFK1
hFK2
hFK3
hFK3-hFK1
Motif MAP: ESRP1-TGGTGG
Motif MAP: RBFOX1/2-[AT]GCATG[AC]
Motif MAP: QKI-ACTAAC[ACG]
-log(pVal) up vs. bg
-log(pVal) dn vs. bg
Upregulated
Downregulated
Background
Motif Score (mean)
Negative log10(pValue)

◂**Figure 4.** RNA binding motif enrichment analysis indicates that the mRNA binding proteins ESRP1, ESRP2, RBFOX2, and QKI regulate alternative mRNA splicing during human kidney development. (**A**) Shown is a comparison of gene expression levels of 89 known RNA binding proteins between hFK1 and hFK3 (see "Materials and methods"). (**B**) RNA binding motif enrichment analysis using rMAPS identifies four putative splicing factors: ESRP1, ESRP2 (see Fig. S5A), RBFOX2, and QKI. ESRP1 and ESRP2 have low expression levels in all Wilms' tumor samples and monotonically increase along kidney development, starting with moderate levels in hFK1 and reaching a maximum in hFK3. Likewise, exons that were enhanced in hFK3 (with respect to hFK1) are enriched for ESRP1 binding sites at their downstream 3' flanking intron (red curve), while exons that are silenced in hFK3 are enriched for ESRP1 binding sites at their upstream 5′ flanking intron (blue curve). On the other hand, RBFOX2 shows a monotonic decrease in expression levels along kidney development, starting with high levels in hFK1 and decreasing in hFK2 and hFK3 (see discussion). Exons that are elevated in hFK1 (with respect to hFK3) are enriched for RBFOX2 binding sites at their downstream 3′ flanking intron (blue curve). Although QKI did not show a monotonic change in expression levels between hFK1, hFK2, and hFK3, its RNA binding sites show similar behavior to RBFOX2, that is, exons that are elevated in hFK1 (with respect to hFK3) are enriched for QKI binding sites at their downstream 3′ flanking intron (blue curve), and exons that are elevated in hFK3 (with respect to hFK1) are enriched for QKI binding sites at their upstream 5′ flanking intron (red curve). (**C**) These results are consistent with the model for splicing regulation during the Mesenchymal to Epithelial Transition (MET) as proposed by Yang et al.[31]. Applying this model to kidney development, the hFK1 cell fraction corresponds to early kidney developmental stages and is predominantly composed of mesenchymal cells (the cap mesenchyme and the un-induced metanephric mesenchyme). Therefore in hFK1, ESRP1 and ESRP2 are low and RBFOX2 and QKI promote exon inclusion by binding to downstream introns, or exon skipping by binding to upstream introns. The hKF3 fraction corresponds to a late more differentiated kidney developmental stage and is predominantly composed of epithelial cells. As a result, ESRP1 and ESRP2 are high in hFK3 and promote exon inclusion by binding to downstream introns, or exon skipping by binding to upstream introns.

We next chose cassette/skipped exons (SE) that were significantly differentially spliced (FDR < 1E−9 and difference in inclusion levels > 0.1) between hFK1 and hFK3—the cell fractions representing the earliest and latest stages of kidney development—and of these we selected 36 cassette exons that also showed clear alternative splicing by manual inspection in the IGV genome browser[23] (Figs. S7–S35). Hierarchical clustering (Fig. 3A) and barplots (Figs. 3B and S7–S35) of the inclusion levels of these 36 selected cassette exons showed that hFK1, the early-stage fetal fraction, has a splice isoform profile that is similar to the Wilms' tumor xenografts (WT37, WT14, and WT11). Gene Ontology (GO) enrichment analysis for the genes containing these 36 selected cassette exons showed that they are related to mesenchymal or epithelial characteristics (e.g., cell motility or cell to cell junctions, Fig. 3D, Table S9). Moreover, enrichment analysis with respect to gene sets found in previous studies (e.g.[29]) indicated that alternative splicing in these genes is regulated by the RNA binding proteins ESRP1 and ESRP2 (Fig. 3D, Table S9).

We also identified other types of alternative splicing between the cell fractions representing the earliest (hFK1) and latest (hFK3) stages of kidney development, though to a much lesser extent than skipped exons: the genes FGFR2 (Fig. S36, previously known from the literature to be alternatively spliced between mesenchymal and epithelial tissues[35,36]) and FYN (Fig. S37) contain mutually exclusive exons (MXE), the genes CYB561A3 (Fig. S38) and RPS24 (Fig. S39) contain alternative 3' splice-sites (A3SS), the gene CTNND1 (Fig. S40) contains an alternative 5' splice-site (A5SS), and the gene LUC7L3 (Fig. S41) contains a retained intron (RI). For these genes also, the Wilms' tumor xenografts (WT37, WT14, and WT11) expressed splicing isoforms that were more similar to those expressed by hFK1.

We note that we did not find any consistent relationship between gene expression levels and exon inclusion levels within the same gene (Fig. S3): For some genes we observed a very positive correlation (e.g. USO1, in which both expression levels and exon inclusion levels increase during development; $r = 0.83$), while for others we observed a very negative correlation (e.g. ACOT9, in which expression levels increase during development and exon inclusion levels decrease; $r = -0.77$) or no correlation at all (e.g. SLK, in which expression levels are constant while and exon inclusion levels increase during development; $r = 0.086$).

RNA binding motif enrichment analysis indicates that the mRNA binding proteins ESRP1, ESRP2, RBFOX2, and QKI regulate alternative mRNA splicing during human kidney development. Next, we searched among known RNA binding proteins (RBPs) for genes that are likely to be responsible for regulating alternative mRNA splicing during human kidney development[38,39]. Among the genes that we observed to be alternatively spliced are FAT1[8,40] (Figs. S2 and S18) and PLOD2[8,31,41] (Figs. S2 and S24), two genes for which alternative splicing was previously found to be regulated by the RNA binding protein RBFOX2[8], and ARHGEF10L[29,30,42] (Figs. S2 and S10), a gene for which alternative splicing was previously found to be regulated by the RNA binding proteins ESRP1 and ESRP2[29].

In order to conduct a more systematic search, we compared the mean expression levels of 89 known RNA binding proteins[25–27] and found several putative splicing regulators that were differentially expressed between hFK1, the cell fraction representing the early stages of fetal kidney development, and hFK3, the cell fraction representing the latest most differentiated stage (Fig. 4A). We found that ESRP1 and ESRP2 are over-expressed in hFK3 with respect to hFK1 (as well as the Wilms' tumor xenografts WT37, WT14, and WT11; Figs. 4B and S5A). On the other hand, RBFOX2 was found to be over-expressed in hFK1 with respect to hFK3 (Fig. 4B).

We next used rMAPS[27] to perform enrichment analysis for RNA binding sites (motifs) that belong to these known RNA binding proteins (RBPs). We found that the RNA binding sites of ESRP1, ESRP2, and RBFOX2 are enriched in the upstream or downstream flanking introns of the cassette exons that are differentially expressed between hFK1 and hFK3 (Fig. 4B, Fig. S5A)[26,28–31,43]. This indicates that ESRP1, ESRP2, and RBFOX2 are splicing regulators involved in the Mesenchymal to Epithelial Transition (MET) that occurs during human fetal kidney development (Fig. 4C). Another putative regulator is QKI1 which, although does not show an appreciable change in expression levels between hFK1 and hFK3, has an RNA binding site that shows a similar enrichment pattern as RBFOX2[31].

These results are somewhat similar to what was previously observed by Yang et al.[31] in cells from a human H358 epithelial non-small cell lung cancer (NSCLC) cell line undergoing EMT (see comparison in Fig. S4) and consistent with their proposed model for splicing regulation during this transition (Fig. 4C). Applying this model to kidney development, the hFK1 cell fraction corresponds to early kidney developmental stages and is predominantly composed of mesenchymal cells (the cap mesenchyme and the un-induced metanephric mesenchyme). Therefore in hFK1, ESRP1 and ESRP2 are low and RBFOX2 and QKI promote exon inclusion by binding to downstream introns, or exon skipping by binding to upstream introns. The hKF3 fraction corresponds to a later more differentiated kidney developmental stage that is predominantly composed of epithelial cells. As a result, ESRP1 and ESRP2 are high in hFK3 and promote exon inclusion by binding to downstream introns, or exon skipping by binding to upstream introns.

Discussion

In this study, we used "bulk" RNA sequencing in order to comprehensively characterize alternative splicing in cell populations representing early, intermediate, and late developmental stages of the human fetal kidney, as well as three blastemal-predominant Wilms' tumor patient-derived xenografts (WT-PDX) that represent an aggressive subtype of Wilms' tumors. We found a set of transcripts that are alternatively spliced between the different developmental stages and identified putative splicing regulators. Moreover, we found that the blastemal-predominant Wilms' tumor patient-derived xenografts (WT-PDX) resemble the earliest developmental stage in both gene expression and alternative splicing. These results illuminate new molecular mechanisms involved in kidney development, and we anticipate that they may assist in the design of new markers and therapeutic strategies for abnormal kidney development and pediatric kidney tumors.

The kidney is a heterogeneous organ composed of millions of microstructures, each composed of different cell types. Ideally, the best way to characterize alternative splicing throughout the different developmental stages is by applying full transcript length single-cell RNA sequencing[44–47]. We have recently performed full transcript length single-cell RNA sequencing in the developing mouse fetal kidney[48] and identified a set of transcripts—similar to those found here—that undergo alternative mRNA splicing during the transition between mesenchymal and epithelial cellular states that takes place in the course of mouse fetal kidney development. Likewise, RNA binding motif enrichment analysis suggested that Esrp1/2 and Rbfox1/2 are splicing regulators of the Mesenchymal to Epithelial Transition (MET) that occurs during mouse kidney development, also similar to what we found here.

However, single-cell RNA sequencing is costly and often prone to bias and low coverage, which makes alternative splicing analysis challenging. Moreover, human fetal tissues are technically difficult to obtain in a "fresh" and viable state that is suitable for single-cell RNA sequencing. Therefore, for the present study, we deeply sequenced "bulk" RNA from cells that were harvested from primary human fetal tissues, cultured overnight, and enriched by flow cytometry with fluorescently labeled antibodies according to a protocol that we have previously shown to enrich for cell fractions that represent early, intermediate, and late developmental stages of the human fetal kidney[7]. Although some cells types such as podocytes are not preserved during the overnight culturing, we have previously shown[7] that this method does faithfully represent central developmental processes that occur during kidney development such as the Mesenchymal to Epithelial Transition (MET). Likewise, in order to overcome similar difficulties in obtaining "fresh" Wilms' tumor samples, we used patient-derived xenografts (WT-PDX) that were established in the course of previous studies[7,13–16].

We noticed that the Wilms' tumor xenografts have a rather large heterogeneity in both gene expression (Fig. 2A) and mRNA splicing (Fig. 3C). This might be due to the fact that these tumors originated from three different patients and that each has its own unique genetic distortions. It is also likely that although all three xenografts are predominantly blastemal, they also contain varying proportions of minority stromal and epithelial cells. This might also explain the heterogeneity in expression levels of QKI (Fig. 4B), and also the fact that unlike ESRP1 and ESRP2, the expression levels of RBFOX2 in the Wilms' tumor xenograft samples are heterogeneous and not similar to those in hFK1 (Fig. 4B).

We note that RNA binding motif enrichment analysis is currently somewhat limited, probably due to limited knowledge and the fact that many known motifs are typically only a few bases long. This results in non-specific results pointing to candidate splicing regulators that are expressed at low levels in some populations (e.g., RBFOX1, Fig. 4A) or, conversely, in potential splicing regulators that are differentially expressed but for which no motif enrichment is detected. For example, RBM47[31] is differentially over-expressed in hFK3 vs. hFK1 (Figs. 4A, S5B), which indicates that it might also be involved in splicing regulation during kidney development, but we did not find significant motif enrichment for this gene. Similarly, we observed additional RNA binding proteins (Fig. S6) that are differentially expressed between hFK1 and hFK3 or between the Wilms' tumors (WT37, WT14, and WT11) and hFK3, which indicates that they might also be involved in splicing regulation, but we did not find any significant motif enrichment for these genes.

Another limitation of our study is the small number of replicates—three Wilms' tumor xenografts from three patients and three samples (corresponding to three developmental stages) of human fetal kidney cells from a single fetus. This was mainly due to the difficulties involved in obtaining "fresh" human tissues. In order to

mitigate this limitation, we manually inspected each gene in the genome browser (Figs. S7–S42) and chose only those splicing events that are consistent in all samples, i.e., those that are similarly expressed in the three Wilms' tumors (while taking into account that tumors can vary widely from each other) and that can be clearly seen to increase or decrease monotonically with developmental stage in the fetal samples. Nevertheless, we believe that future studies using multiple biological replicates of "fresh" human tissues at the single-cell level, and preferably also supported by isoform-specific qPCR (as was previously shown for the gene ENAH[13]), will be needed to fully characterize alternative splicing in kidney development and Wilms' tumors.

Although in this study we did not perform functional validation, the putative splicing regulators that we identified here (ESRP1, ESRP2, RBFOX2, and QKI) were found to have similar functionality in other developing organs and in-vitro systems[10,28,30,31,35,37,49], as well as in the kidney. For example, a recent study showed that the splicing regulator ESRP2 is repressed in Wilms' tumors by DNA methylation from their very early stages (nephrogenic rests)[50], and that over-expression of ESRP2 in Wilms' tumor cell lines inhibits their proliferation both *in-vitro* and *in-vivo*. Another study showed that Esrp1 ablation in mice, alone or together with Esrp2, results in reduced kidney size, fewer ureteric tips, reduced nephron numbers, and a global reduction of epithelial splice isoforms in the transcriptome of ureteric epithelial cells[51]. These studies indicate that timely expression of ESRP1 and ESRP2 is required for proper mesenchymal to epithelial transition and nephron development. However, the fact that kidneys still develop in mice after Esrp1 and Esrp2 ablation, taken with our results, suggests that other splicing regulators such as Rbfox1, Rbfox2, or Qki can compensate, although partially, for the ablation of Esrp1 and Esrp2.

Data availability

The GEO series record for the RNA sequencing data is: GSE150684.

Received: 17 December 2020; Accepted: 10 November 2022
Published online: 15 November 2022

References

1. Hohenstein, P., Pritchard-Jones, K. & Charlton, J. The yin and yang of kidney development and Wilms' tumors. *Genes Dev.* **29**, 467–482. https://doi.org/10.1101/gad.256396.114 (2015).
2. Little, M., Georgas, K., Pennisi, D. & Wilkinson, L. Kidney Development: two tales of tubulogenesis. In *Current Topics in Developmental Biology* (eds Thornhill, B. A., & Chevalier, R. L.) 193–229 (2010) https://doi.org/10.1016/S0070-2153(10)90005-7.
3. Gilbert, S. F. *Developmental Biology*. 6th ed. (Sinauer Associates, 2000). Intermediate Mesoderm. https://www.ncbi.nlm.nih.gov/books/NBK10089/.
4. Davidoff, A. M. Wilms tumor. *Adv. Pediatr.* **59**, 247–267. https://doi.org/10.1016/j.yapd.2012.04.001 (2012).
5. Huff, V. Wilms' tumours: About tumour suppressor genes, an oncogene and a chameleon gene. *Nat. Rev. Cancer.* **11**, 111–121. https://doi.org/10.1038/nrc3002 (2011).
6. Popov, S. D., Sebire, N. J. & Vujanic, G. M. Wilms' tumour—histology and differential diagnosis. In *Wilm Tumor* (ed van den Heuvel-Eibrink, M. M) (2016) https://doi.org/10.15586/codon.wt.2016.ch1.
7. Pode-Shakked, N. *et al.* Dissecting stages of human kidney development and tumorigenesis with surface markers affords simple prospective purification of nephron stem cells. *Sci. Rep.* **6**, 23562. https://doi.org/10.1038/srep23562 (2016).
8. Shapiro, I. M. *et al.* An EMT-driven alternative splicing program occurs in human breast cancer and modulates cellular phenotype. *PLoS Genet.* https://doi.org/10.1371/journal.pgen.1002218 (2011).
9. Di Modugno, F. *et al.* Splicing program of human MENA produces a previously undescribed isoform associated with invasive, mesenchymal-like breast tumors. *Proc. Natl. Acad. Sci. USA.* **109**, 19280–19285. https://doi.org/10.1073/pnas.1214394109 (2012).
10. Warzecha, C. C., Shen, S., Xing, Y. & Carstens, R. P. The epithelial splicing factors ESRP1 and ESRP2 positively and negatively regulate diverse types of alternative splicing events. *RNA Biol.* **6**, 546–562. https://doi.org/10.4161/rna.6.5.9606 (2009).
11. Sneath, R. J. & Mangham, D. C. The normal structure and function of CD44 and its role in neoplasia. *Mol. Pathol.* **51**, 191–200. https://doi.org/10.1136/mp.51.4.191 (1998).
12. Brown, R. L. *et al.* CD44 splice isoform switching in human and mouse epithelium is essential for epithelial-mesenchymal transition and breast cancer progression. *J. Clin. Investig.* **121**, 1064–1074. https://doi.org/10.1172/JCI44540 (2011).
13. Pode-Shakked, N. *et al.* Evidence of in vitro preservation of human nephrogenesis at the single-cell level. *Stem Cell Rep.* https://doi.org/10.1016/j.stemcr.2017.04.026 (2017).
14. Metsuyanim, S. *et al.* Expression of stem cell markers in the human fetal kidney. *PLoS ONE* https://doi.org/10.1371/journal.pone.0006709 (2009).
15. Pode-Shakked, N. *et al.* The isolation and characterization of renal cancer initiating cells from human Wilms' tumour xenografts unveils new therapeutic targets. *EMBO Mol. Med.* **5**, 18–37. https://doi.org/10.1002/emmm.201201516 (2013).
16. Pode-Shakked, N. *et al.* Developmental tumourigenesis: NCAM as a putative marker for the malignant renal stem/progenitor cell population. *J. Cell Mol. Med.* **13**, 1792–1808 (2009).
17. Kim, D. *et al.* TopHat2: Accurate alignment of transcriptomes in the presence of insertions, deletions and gene fusions. *Genome Biol.* **14**, R36. https://doi.org/10.1186/gb-2013-14-4-r36 (2013).
18. Anders, S., Pyl, P. T. & Huber, W. HTSeq-A Python framework to work with high-throughput sequencing data. *Bioinformatics* **31**, 166–169. https://doi.org/10.1093/bioinformatics/btu638 (2015).
19. Love, M. I., Huber, W. & Anders, S. Moderated estimation of fold change and dispersion for RNA-seq data with DESeq2. *Genome Biol.* **15**, 550. https://doi.org/10.1186/s13059-014-0550-8 (2014).
20. Chen, J., Bardes, E. E., Aronow, B. J. & Jegga, A. G. ToppGene Suite for gene list enrichment analysis and candidate gene prioritization. *Nucleic Acids Res.* https://doi.org/10.1093/nar/gkp427 (2009).
21. Subramanian, A., Tamayo, P., Mootha, V. K., Mukherjee, S. & Ebert, B. L. Gene set enrichment analysis: A knowledge-based approach for interpreting genome-wide. *Proc. Natl. Acad. Sci. USA* **102**, 15545–15550 (2005).
22. Shen, S. *et al.* rMATS: Robust and flexible detection of differential alternative splicing from replicate RNA-Seq data. *Proc. Natl. Acad. Sci. USA.* **111**, E5593–E5601. https://doi.org/10.1073/pnas.1419161111 (2014).
23. Thorvaldsdóttir, H., Robinson, J. T. & Mesirov, J. P. Integrative Genomics Viewer (IGV): High-performance genomics data visualization and exploration. *Brief Bioinform.* **14**, 178–192. https://doi.org/10.1093/bib/bbs017 (2013).
24. Katz, Y. *et al.* Quantitative visualization of alternative exon expression from RNA-seq data. *Bioinformatics* **31**, 2400–2402. https://doi.org/10.1093/bioinformatics/btv034 (2015).
25. Park, J. W., Jung, S., Rouchka, E. C., Tseng, Y. T. & Xing, Y. rMAPS: RNA map analysis and plotting server for alternative exon regulation. *Nucleic Acids Res.* **44**, W333–W338. https://doi.org/10.1093/nar/gkw410 (2016).

26. Ray, D. *et al.* A compendium of RNA-binding motifs for decoding gene regulation. *Nature* **499**, 172–177. https://doi.org/10.1038/nature12311 (2013).
27. Anderson, E. S. *et al.* The cardiotonic steroid digitoxin regulates alternative splicing through depletion of the splicing factors SRSF3 and TRA2B. *RNA* **17**, 1041–1049. https://doi.org/10.1261/rna.032912.112 (2012).
28. Dittmar, K. A. *et al.* Genome-wide determination of a broad ESRP-regulated posttranscriptional network by high-throughput sequencing. *Mol. Cell Biol.* **32**, 1468–1482. https://doi.org/10.1128/MCB.06536-11 (2012).
29. Bebee, T. W. *et al.* The splicing regulators Esrp1 and Esrp2 direct an epithelial splicing program essential for mammalian development. *Elife* **4**, 1–27. https://doi.org/10.7554/eLife.08954 (2015).
30. Bhate, A. *et al.* ESRP2 controls an adult splicing programme in hepatocytes to support postnatal liver maturation. *Nat. Commun.* **6**, 8768. https://doi.org/10.1038/ncomms9768 (2015).
31. Yang, Y. *et al.* Determination of a comprehensive alternative splicing regulatory network and combinatorial regulation by key factors during the epithelial-to-mesenchymal transition. *Mol. Cell Biol.* **36**, 1704–1719. https://doi.org/10.1128/MCB.00019-16 (2016).
32. Brunskill, E. W. *et al.* Atlas of gene expression in the developing kidney at microanatomic resolution. *Dev. Cell* **15**, 781–791. https://doi.org/10.1016/j.devcel.2008.09.007 (2008).
33. Magella, B. *et al.* Cross-platform single cell analysis of kidney development shows stromal cells express Gdnf. *Dev. Biol.* **434**, 1–12. https://doi.org/10.1016/j.ydbio.2017.11.006 (2017).
34. Adam, M., Potter, A. S. & Potter, S. S. Psychrophilic proteases dramatically reduce single cell RNA-seq artifacts: A molecular atlas of kidney development. *Development* **1**, dev.151142. https://doi.org/10.1242/dev.151142 (2017).
35. Warzecha, C. C., Sato, T. K., Nabet, B., Hogenesch, J. B. & Carstens, R. P. ESRP1 and ESRP2 are epithelial cell-type-specific regulators of FGFR2 splicing. *Mol. Cell* **33**, 591–601. https://doi.org/10.1016/j.molcel.2009.01.025 (2009).
36. Hovhannisyan, R. H., Warzecha, C. C. & Carstens, R. P. Characterization of sequences and mechanisms through which ISE/ISS-3 regulates FGFR2 splicing. *Nucleic Acids Res.* **34**, 373–385. https://doi.org/10.1093/nar/gkj407 (2006).
37. Warzecha, C. C. & Carstens, R. P. Complex changes in alternative pre-mRNA splicing play a central role in the epithelial-to-mesenchymal transition (EMT). *Semin Cancer Biol.* **22**, 417–427. https://doi.org/10.1016/j.semcancer.2012.04.003 (2012).
38. Wang, Z. & Burge, C. B. Splicing regulation: From a parts list of regulatory elements to an integrated splicing code. *RNA* **14**, 802–813. https://doi.org/10.1261/rna.876308.802 (2008).
39. Wang, E. T. *et al.* Alternative isoform regulation in human tissue transcriptomes. *Nature* **456**, 470–476. https://doi.org/10.1038/nature07509 (2008).
40. Braeutigam, C. *et al.* The RNA-binding protein Rbfox2: An essential regulator of EMT-driven alternative splicing and a mediator of cellular invasion. *Oncogene* **33**, 1082–1092. https://doi.org/10.1038/onc.2013.50 (2014).
41. Yeowell, H. N. & Walker, L. C. Tissue specificity of a new splice form of the human lysyl hydroxylase 2 gene. *Matrix Biol.* **18**, 179–187. https://doi.org/10.1016/S0945-053X(99)00013-X (1999).
42. Bangru, S. *et al.* Alternative splicing rewires Hippo signaling pathway in hepatocytes to promote liver regeneration. *Nat. Struct. Mol. Biol.* **25**, 928–939. https://doi.org/10.1038/s41594-018-0129-2 (2018).
43. Jin, Y. *et al.* A vertebrate RNA-binding protein Fox-1 regulates tissue-specific splicing via the pentanucleotide GCAUG. *EMBO J.* **22**, 905–912. https://doi.org/10.1093/emboj/cdg089 (2003).
44. Picelli, S. *et al.* Tn5 transposase and tagmentation procedures for massively scaled sequencing projects. *Genome Res.* **24**, 2033–2040. https://doi.org/10.1101/gr.177881.114 (2014).
45. Picelli, S. *et al.* Smart-seq2 for sensitive full-length transcriptome profiling in single cells. *Nat. Methods.* **10**, 1096–1098. https://doi.org/10.1038/nmeth.2639 (2013).
46. Shalek, A. K. *et al.* Single-cell transcriptomics reveals bimodality in expression and splicing in immune cells. *Nature* **498**, 236–240. https://doi.org/10.1038/nature12172.Single-cell (2013).
47. Brunskill, E. W. *et al.* Single cell dissection of early kidney development: Multilineage priming. *Development* **141**, 3093–3101. https://doi.org/10.1242/dev.110601 (2014).
48. Wineberg, Y. *et al.* Single-cell RNA sequencing reveals mRNA splice isoform switching during kidney development. *J. Am. Soc. Nephrol.* https://doi.org/10.1681/ASN.2019080770 (2020).
49. Warzecha, C. C. *et al.* An ESRP-regulated splicing programme is abrogated during the epithelial-mesenchymal transition. *EMBO J.* **29**, 3286–3300. https://doi.org/10.1038/emboj.2010.195 (2010).
50. Legge, D. *et al.* The epithelial splicing regulator ESRP2 is epigenetically repressed by DNA hypermethylation in Wilms tumour and acts as a tumour suppressor. *Mol. Oncol.* **16**, 630–647. https://doi.org/10.1002/1878-0261.13101 (2022).
51. Bebee, T. W. *et al.* Ablation of the epithelial-specific splicing factor Esrp1 results in ureteric branching defects and reduced nephron number. *Dev. Dyn.* **245**, 991–1000. https://doi.org/10.1002/dvdy.24431 (2016).

Acknowledgements

We wish to thank Jordan Kreidberg, Steve Potter, Oded Volovelsky, Morris Nehama, Tal Shay, Rotem Karni, Peter Hohenstein, the anonymous reviewers of this manuscript, and all members of our labs for useful comments and suggestions.

Author contributions

Study initiation and conception—Y.W., I.K., N.B.H., E.B., N.P.S., B.D., and T.K.; Human Fetal kidney collection, culturing, sorting, and RNA extraction—N.P.S. and R.G.; Wilms' tumor patient-derived xenograft (WT-PDX) maintenance, collection, culturing, and RNA extraction—N.P.S., R.G, R.S., and D.D.B.L.; RNA quality checks—E.B. and T.H.B.L.; RNA sequence preprocessing—I.K., N.B.H., and E.B.; Gene expression and splicing analysis—Y.W., I.K., E.B., N.B.H., H.R., and T.K.; Other intellectual contribution—S.O., Y.Y., and A.U.; Manuscript writing—Y.W., I.K., and T.K.

Funding

Y.W., I.K., N.B.H., E.B., T.H.B.L., S.O., H.R., Y.Y., and T.K., were supported by the Israel Science Foundation (ICORE no. 1902/12 and Grants no. 1634/13 and 2017/13), the Israel Cancer Association (Grant no. 20150911), the Israel Ministry of Health (Grant no. 3-10146), the EU-FP7 (Marie Curie International Reintegration Grant no. 618592), the Data Science Institute at Bar-Ilan University, and the ICRF (Grant no. 19-101-PG). N.P.S and B.D were supported by the Israel Scientific Foundation (Grant nos. 2071/17 and 910/11). The funders had no role in study design, data collection and analysis, decision to publish, or preparation of the manuscript.

Competing interests
The authors declare no competing interests.

Additional information
Supplementary Information The online version contains supplementary material available at https://doi.org/10.1038/s41598-022-24147-z.

Correspondence and requests for materials should be addressed to T.K.

Reprints and permissions information is available at www.nature.com/reprints.

Publisher's note Springer Nature remains neutral with regard to jurisdictional claims in published maps and institutional affiliations.